Microstructural characterization of laser cladding of Cu-30Ni

BIJAYA ADAK*, PHILIP NASH, DAJUN CHEN
Thermal Processing Technology Center, Illinois Institute of Technology, Chicago, IL 60616, USA

ALAN SWIGLO
Alion Science and Technology, St. Charles, IL 60174, USA

Cu-Ni alloys are known for their corrosion resistant properties and one of the important applications of these alloys is in marine components. Such components can be subject to wear resulting ultimately in failure. Refurbishment of such worn components, particularly *in situ*, would provide a cost-effective alternative to complete replacement. One such method proposed for refurbishment of large marine components is laser cladding. The successful application of this technique requires some research to establish the optimum processing parameters to be used for particular combinations of substrate and clad materials. We have been investigating the laser cladding of Cu-30Ni alloy plates with a diode laser in order to establish the microstructure of the clad material and the heat affected zone in the substrate as a function of the process parameters. This paper reports on various microstructural observations of these clads and discusses certain undesired features encountered.

In the present study, a diode laser (Nuvonyx–ISL system with max. power 4 kW) was used as the heat source. The laser beam has a rectangular cross section which at the focal length is 12 mm $\times$ 0.5 mm. A diode laser was chosen since it has the highest output efficiency (ratio of output power to input power) compared to other laser sources such as CO_2 or YAG laser. Commercially available Cu-30Ni alloy was used for both substrate and filler material. The substrate plates were 19 mm thick and wires of 0.89 mm diameter were used for the filler material. Chemical compositions for the cladding material and substrate are shown in Table I. The melting temperature range for the alloy from the phase diagram [4] is 1170–1240 °C. Cu-30Ni alloy exhibits complete solid solubility down to around 200 °C where the phase separation is kinetically constrained due to the low temperature and rapid heat extraction, consequently a single phase microstructure is expected in these laser cladding studies.

The microstructure was evaluated with respect to different process parameters: laser power, laser translation speed, wire feed rate and beam angle (angle between the beam and travel direction over the substrate). The range of these parameters is given in Table II. The microstructures were characterized using optical microscopy, X-ray diffraction and EDS (Energy Dispersive Spectrometer) analysis. No clear relationship between solidification and process parameters was observed for the range of process parameters used, as all the samples showed similar solidification behavior. Solidification starts from partially melted substrate without any sharp interface (Fig. 1). The partially melted interface region is about 50 μm in width.

As we know the temperature range between the liquid and the solid state for this alloy is 70 °C we can calculate the temperature gradient in this region as 1400 °C/mm. Rapid solidification occurs in the melted substrate and clad material. This is clear from the fine secondary dendrite arm spacing in the dendritic solidification regions (Fig. 2) and the appearance of a cellular type solidification close to the interface with the unmelted substrate (Fig. 1). In all the samples, prepared with the range of parameters, the microstructure is mostly dendritic (Fig. 2) and a thin layer of cellular type solidification was observed at the interface (Fig. 1). Competitive growth of solid nuclei leads to preferential growth of certain grains. In cubic materials it is commonly observed that the [1 0 0] direction will exhibit the fastest growth. In such a case one would expect a strong (1 0 0) texture to develop in the clad and this is observed from the X-ray diffraction pattern of the region close to the top of the clad material (Fig. 3), where the (2 0 0) peak is significantly stronger than the (1 1 1) peak. For comparison, the intensities for pure nontextured Cu are shown by the dashed vertical lines. The X-ray diffraction pattern of the substrate, (Fig. 4), exhibits peak intensities consistent with a nontextured diffraction pattern. Lattice parameters of the base and clad materials were calculated based on the peak positions from the X-ray diffraction patterns. The lattice parameter for the substrate is 0.3581 nm and for the clad material is 0.3585 nm. These values are consistent with the expected values based on the Cu and Ni content [4] of the material. Both the diffraction patterns show the presence of the face centered cubic, copper based alloy with only one additional peak in the clad which was identified as Cu_2O.

Although shielding gas (argon) was used to prevent oxide formation, a weak peak at 36° on the XRD pattern of the clad indicates the presence of cuprous oxide (Cu_2O). EDS analysis of the top surface of the clad also shows the presence of oxides. This could be the result of incomplete coverage by the argon shielding

*Author to whom all correspondence should be addressed.

0022–2461

TABLE I Chemical composition wt.(%)

Element	Wire	Substance
Cu	Balance	Balance
Ni	28–82	29.37
Fe	0.66	0.86
Mn	0.72	0.78
Ti	0.4	0.2
Pb	0	<0.01
Zn	<0.01	0.02
O_2[a]	61	14

[a]In ppm.

TABLE II Process parameter's range

Process parameter	Range
Laser power (kW)	3–4
Laser translation speed (mm/s)	2.25–6.85
Wire feeding speed (mm/s)	29–75
Beam angle (°)	22.5–90

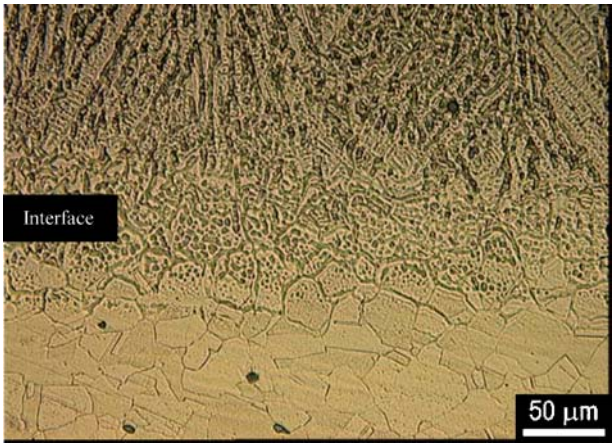

Figure 1 Interface region between melted and unmelted substrate of Cu-30Ni.

gas or due to the release of dissolved oxygen in the filler and base material. As the temperature decreases during solidification, the maximum tolerable oxygen partial pressure to prevent oxide formation decreases. Since the partition coefficient for this copper rich alloy is greater than 1, we can expect copper rich liquid to solidify last at the surface of the clad at around 1170 °C. Etching with copper sulfate and hydrochloric acid (ASTM standard: E 407–93, etchant # 25, [6]) reveals the presence of interdendritic segregation (Fig. 1). EDS analysis shows that the interdendritic region is Cu rich and the core is Ni rich as expected from the phase diagram. This copper rich region can oxidize during cooling after solidification. Fig. 5 represents the stability of Cu and various Cu oxides below 1200 K. As Cu_2O was formed rather than CuO we know that the oxygen partial pressure locally at the clad surface was between the two curves for oxide formation as seen from Fig. 5. If we assume that the kinetics of oxide formation are too low below 1000 K we can estimate the oxygen partial pressure range that existed. On this basis we can say that the oxygen partial pressure range was

Figure 2 Dendritic solidification of Cu-30Ni clad material and melted substrate with strong (1 0 0) texture.

between 3.5×10^{-11} and 6.6×10^{-5} atm. This could quite easily occur behind the melt zone since the cover gas is injected from a nozzle which moves with the laser beam.

Segregation of titanium and manganese in the form of small beads was also observed along one of the clad edges. This edge corresponded to the edge furthest from the gas shielding nozzle. The composition of these beads was variable but consisted mostly of Ti and Mn in a ratio of approximately 30% Ti and 60% Mn. This appears to correspond to $TiMn_2$ which melts at 1325 °C. This compound formed a slag since it has a lower density and higher melting point than the Cu-Ni alloy and was pushed across the surface of the liquid clad material by the gas flow. Shrinkage porosity due to dendritic solidification was observed in the clad and resolidified base material (Fig. 6). Large gas bubbles were observed, mostly near the surface of the clad layer. These bubbles could result from either entrapped shielding gas or evolved oxygen on solidification of the Cu-Ni alloy. As such clads would be machined to final size surface bubbles are not likely to pose a problem for the integrity of the clad. No cracks or debonding of the clad material are observed in the interface region.

Experiments were performed over a range of process parameters. Clads showed that microstructure of various samples are independent of the process parameters. Hence, the results of the microstrucutral characterization of laser clad Cu-30Ni alloys using different process parameters indicate that high integrity clads can be produced within a wide range of process parameters. This suggests that the process can

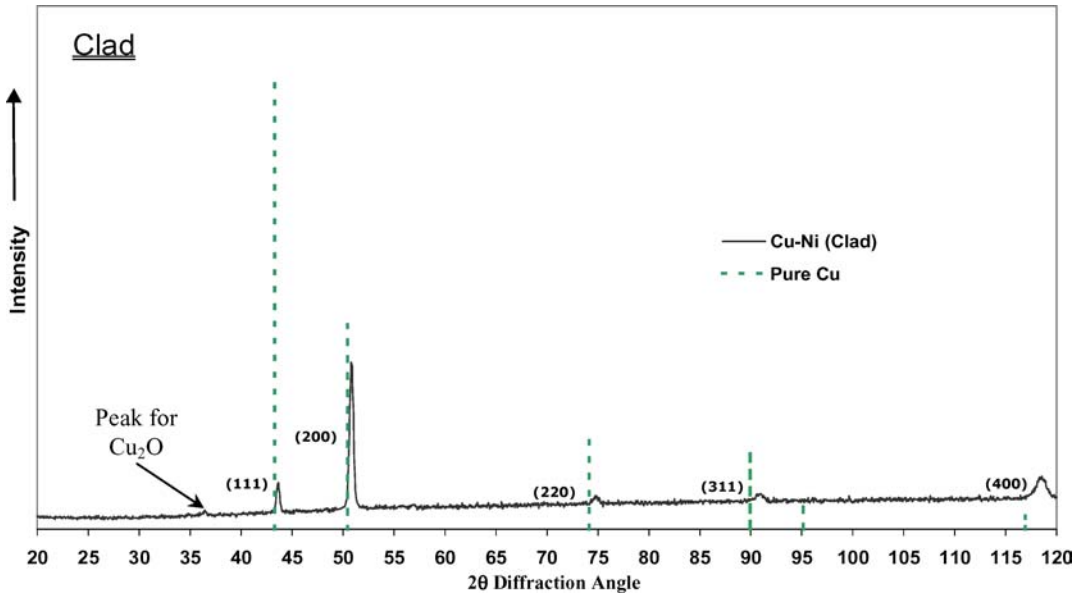

Figure 3 XRD pattern of the clad.

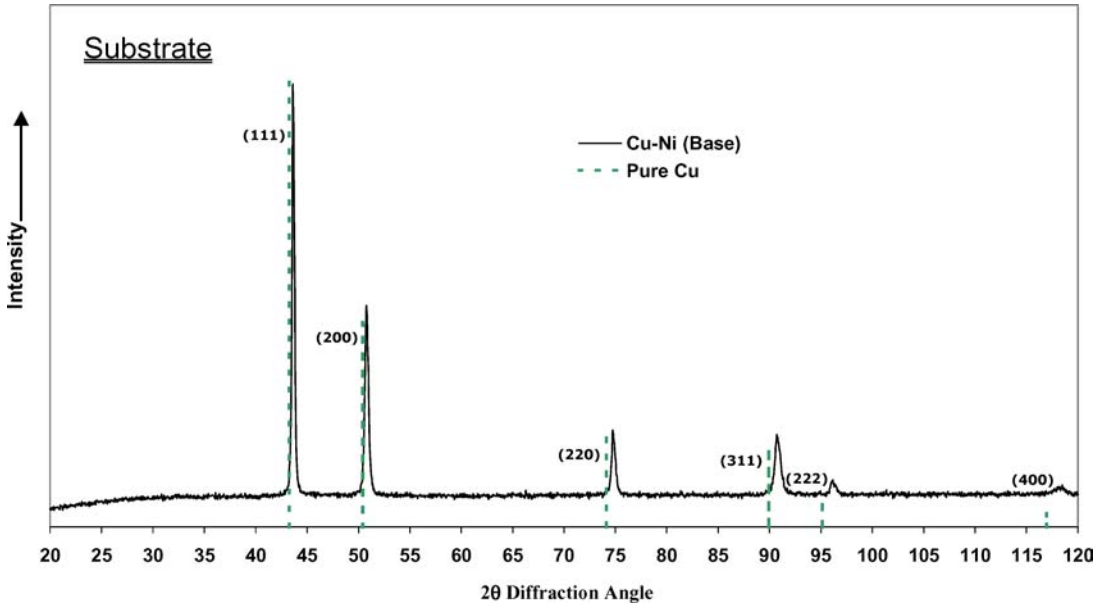

Figure 4 XRD pattern of the substrate.

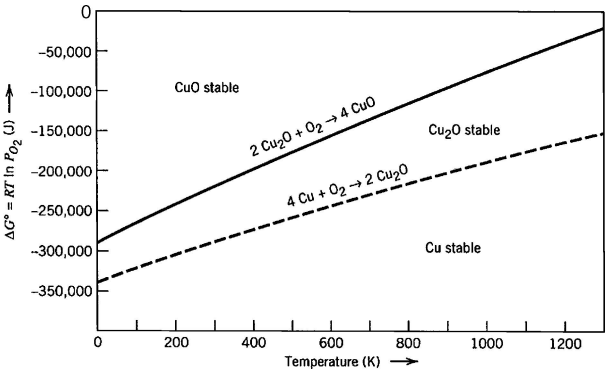

Figure 5 ΔG_0 versus T for oxides of copper, showing regions of stability for Cu, Cu_2O, and CuO (source: Ref. [5]).

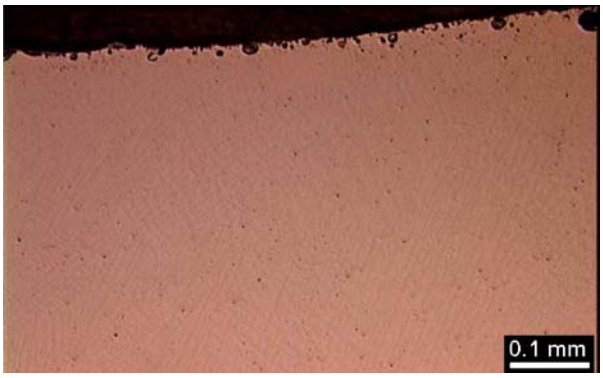

Figure 6 Gas bubbles and shrinkage porosity on the Cu-30Ni clad.

be readily adopted for refurbishing components *in situ* because of the lack of sensitivity to the process parameters which are less controllable in the field than in the laboratory.

References

1. R. VILAR, "Laser Cladding," *J. Laser Appl.* **11**(2) (1999) 64–79.
2. H. GEDDA, "Laser Surface Cladding: A Literature Survey," Technical Report 2000:07, Lulea Technical University, Sweden, 2000.

3. J. HAAKE and M. ZEDIKER, "Laser Processing," *Adv. Mater. & Proc*. (October) 2000, 35–37.
4. D. J. CHAKRABARTI, S. W. LAUGHLIN, S. W. CHEN and Y. A. CHANG, "Cu-Ni (Copper-Nickel)" Phase Diagram of Binary Nickel Alloys", ASM International, June 1991.
5. V. DAVID RAGONE, "Thermodynamics of Materials" (John Wiley & Sons, Inc., 1995), 128 pp.
6. "Annual Book of ASTM Standards," 1994, Section 3, 444 pp.

Received 23 August
and accepted 4 October 2004